

ORIGINAL RESEARCH



KLF4 promotes sevoflurane-induced neurotoxicity by suppressing FOXO1 expression in neonatal rats

Jingjing Hu¹, Yuanfang Li¹, Guoqiang Fei^{1,*}

¹Department of Neurology, Zhongshan Hospital (Xiamen), Fudan University, 361000 Xiamen, Fujian, China

***Correspondence**

Feiguoqiang886@163.com

(Guoqiang Fei)

Abstract

Background: Exposure to anesthetics such as sevoflurane (SEV) during early development has been associated with neurotoxicity. Krüppel-like factor 4 (KLF4), a transcription factor implicated in neuronal injury, has been suggested to play a role in this process. However, the underlying mechanisms remain inadequately characterized. **Methods:** *In vivo*, neonatal rats were intravenously administered adeno-associated virus (AAV) constructs with or without 3% SEV exposure. Their neurological functions were evaluated, and hippocampal tissues were harvested for molecular and histopathological analyses, including NISSL staining, hematoxylin and eosin (H&E) staining, modified Bielschowsky silver staining, Reverse Transcription Quantitative Polymerase Chain Reaction (RT-qPCR), western blotting, Terminal deoxynucleotidyl transferase dUTP Nick End Labeling (TUNEL) assay, oxidative stress assessment and dihydroethidium (DHE) staining. Behavioral assessment was conducted using the Morris water maze (MWM). *In vitro*, HT22 hippocampal neurons were transfected with KLF4-targeting Small Interfering RNAs (siRNAs) and exposed to 3% SEV to assess changes in cell morphology, apoptosis and oxidative stress. **Results:** Sevoflurane exposure led to significant neurotoxicity in neonatal rats, characterized by cognitive impairment, neuronal apoptosis, and oxidative stress, accompanied by increased KLF4 and decreased Forkhead Box Protein O1 (FOXO1) expression. The knockdown of KLF4 using Short Hairpin RNA (shRNA) reversed these effects, improving cognitive performance and reducing neuronal damage and oxidative stress. *In vitro*, KLF4 silencing was found to mitigate SEV-induced cellular injury in HT22 cells. Notably, KLF4 knockdown upregulated FOXO1 expression, which further attenuated SEV-induced apoptosis and oxidative stress. **Conclusions:** These findings indicate that KLF4 aggravates sevoflurane-induced neurotoxicity in neonatal rats by downregulating FOXO1.

Keywords

Neonatal rats; KLF4; FOXO1; Sevoflurane; Neurotoxicity

1. Introduction

Although some studies have reported potential neuroprotective effects of anesthetics, more recent investigations have raised significant concerns regarding their safety, particularly in neonatal animals [1, 2]. Numerous studies have consistently demonstrated increased neuronal apoptosis in the brains of small rodents shortly after exposure to various inhalation anesthetics, including isoflurane and sevoflurane (SEV) [3]. In addition to these acute effects, long-term neurological impairments have been observed in neonates following SEV exposure, suggesting that anesthetics may disrupt normal neurodevelopment [4]. Nerve injury during early life is frequently associated with neuronal apoptosis, synaptic dysfunction, and oxidative stress, all of which contribute to long-term cognitive and behavioral impairments. These outcomes present serious

challenges for modern healthcare, particularly in the field of pediatric anesthesia and neurodevelopment. A growing body of evidence has demonstrated that anesthetic exposure during the neonatal period can lead to neuropathological changes, persistent behavioral abnormalities, and cognitive dysfunction. In rodent models, exposure to various anesthetics during peak synaptogenesis has been shown to alter spontaneous behaviors and impair learning and memory performance [5–7].

SEV is currently the most commonly used inhalational anesthetic in clinical practice. Previous studies have shown that SEV, when administered at concentrations ranging from 2.5% to 4% for 2–6 hours, induces neurotoxicity and cognitive dysfunction in neonatal mice [8–10]. However, the molecular mechanisms underlying this neurotoxicity remain incompletely understood. Krüppel-like factors (KLFs) comprise a family of 17 transcription factors, each characterized by a

highly conserved C-terminal DNA-binding domain containing three Acetylene (C_2H_2) zinc fingers [11]. Among them, KLF4 has been found to play numerous regulatory roles in cell proliferation, differentiation, apoptosis and development. It has been reported that hydrogen peroxide (H_2O_2) induces apoptosis in retinal ganglion cells *in vitro* by upregulating KLF4 expression, while KLF4 knockdown alleviates neuronal damage in traumatic brain injury models through the regulation of p53 and Janus Kinase (JAK)-Signal Transducer and Activator of Transcription 3 (STAT3) signaling pathways [12]. In support of a role in anesthetic-induced neurotoxicity, Yamamoto *et al.* [13] reported increased KLF4 expression in the brains of eight-week-old mice exposed to SEV.

Forkhead box transcription factor O1 (FOXO1) is a key regulator of diverse cellular processes, including gluconeogenesis, adipogenesis, food intake, autophagy and cell cycle arrest [14]. Recent studies have shown that FOXO1 protein expression is significantly reduced in SEV-anesthetized animals compared with controls. Additionally, FOXO1-p21 signaling has been implicated in macrophage polarization during SEV-induced postoperative cognitive dysfunction [15]. Previous findings also suggest that KLF4 can function as a transcriptional repressor of FOXO1, and that suppression of FOXO1 by KLF4 contributes to glioma progression [16].

However, the interaction between KLF4 and FOXO1 in the context of SEV-induced neuronal damage remains poorly characterized. Considering the potential relevance of this pathway, the present study aimed to investigate the role of KLF4 in SEV-induced neurotoxicity and to explore whether this effect involves the regulation of FOXO1, using both *in vivo* and *in vitro* models.

2. Material and methods

2.1 Animal modeling and grouping

All animal procedures were conducted in accordance with the guidelines for the care and use of laboratory animals established by the National Institutes of Health and were approved by the Experimental Animal Ethics Committee of Zhongshan Hospital, Fudan University (Approval No. 20221109-002). The experiment was performed in May 2022 and completed within approximately one week, with all procedures finalized by postnatal day 7 (P7). Sprague Dawley (SD) neonatal rats (2 days old) were purchased from Junke Biological Co., Ltd. (Nanjing, China). The animals were housed at 23 ± 2 °C under a 12-h light/dark cycle with ad libitum access to food and water. A total of 12 neonatal rats were randomly assigned to two groups: sham ($n = 6$) and SEV ($n = 6$). Rats in the SEV group were exposed to 3% SEV in a transparent chamber ($20 \times 12 \times 10$ cm) with a gas mixture containing 30% oxygen balanced with nitrogen for 2 hours [17]. The sham group was exposed to the carrier gas mixture under identical conditions but without SEV. Following exposure, animals were allowed to recover in 30% oxygen for 20 minutes before being returned to their cages. All animals were euthanized on postnatal day 7 (P7). The hippocampus was rapidly dissected from each pup and stored at -80 °C for subsequent analyses.

2.2 KLF4 knockdown

To investigate the role of KLF4 in SEV-induced neurotoxicity, adeno-associated virus (AAV) vectors were used to achieve stable and efficient knockdown of KLF4 in the neonatal rat brain. A total of 24 male neonatal rats were randomly assigned to four groups ($n = 6$ per group): sham + AAV-sh-negative control (NC), sham + AAV-sh-KLF4, SEV + AAV-sh-NC, and SEV + AAV-sh-KLF4. Recombinant AAV serotype 9 vectors encoding either a negative control shRNA (AAV-sh-NC) or shRNA targeting KLF4 (AAV-sh-KLF4) were purchased from Virovek Inc. To ensure efficient knockdown, AAVs were administered prior to SEV exposure. On postnatal day 2 (P2), neonatal rats were intravenously injected with AAVs encoding sh-NC or sh-KLF4. After 48 hours (P4), rats were exposed to 3% SEV or sham conditions for 2 hours to induce neurotoxicity. Following exposure and a 20-minute recovery period in 30% oxygen, AAVs (7.5×10^{11} copies) were injected intravenously. On postnatal day 7 (P7), all animals were euthanized, and the hippocampus was harvested and stored at -80 °C for further analysis [18].

2.3 Neurological function score

Neurological function was evaluated on post-anesthesia day 3 using two behavioral tests: body righting reflex and negative geotaxis to assess early neurodevelopmental impairments after SEV exposure and KLF4 knockdown.

2.4 NISSL staining

Paraffin-embedded hippocampal tissues were sectioned at a thickness of $4 \mu\text{m}$ using a Leica microtome (Leica RM2265, Leica, Wetzlar, HE, Germany) and thoroughly dewaxed in xylene. The sections were then rehydrated through a graded ethanol series (absolute ethanol, 90% ethanol and 70% ethanol). Following rehydration, the sections were stained with NISSL staining solution for 5 minutes. After staining, the samples were rinsed twice with distilled water for a few seconds each. NISSL-positive (NISSL⁺) cells were counted in five randomly selected areas under a light microscope.

2.5 H&E staining

After the same preparatory steps as described in the NISSL staining procedure, the sections were sequentially stained with hematoxylin for 5 minutes and eosin for 3 minutes, according to standard histological protocols. Histopathological abnormalities were then evaluated under an optical microscope (RM2245, Leica, Heidelberg, BW, Germany).

2.6 Modified Bielschowsky silver staining

Modified Bielschowsky silver staining was conducted based on a previously published protocol [19]. Briefly, tissue sections prepared as in the NISSL staining procedure were immersed in a 2–4% silver nitrate solution for 25–35 minutes at 37 °C in the dark. After discarding the silver nitrate solution, the sections were washed three times with distilled water. Deoxygenation was achieved using 10% formaldehyde, followed by three additional rinses with distilled water. The excess

water was removed, and the sections were then incubated with 200 μL of Bielschowsky silver staining reagent for 5 minutes. Subsequently, the sections were treated with 8% formalin for 2 minutes and fixed in 5% sodium thiosulfate for 5 minutes. After air drying and xylene removal, the stained sections were examined microscopically.

2.7 RT-qPCR

Total RNA was extracted from hippocampal brain tissues using TRIzol reagent and reverse-transcribed into complementary DNA (cDNA) using the Quantscript RT Kit (KR103, Tiangen, Beijing, China) following the manufacturer's instructions. Quantitative PCR (qPCR) was performed using the FastFire qPCR PreMix (SYBR Green) (FP209, Tiangen, Beijing, China) on an ABI 7500 Real-Time PCR system (1855195, Bio-RAD, Hercules, CA, USA) to quantify the mRNA levels of KLF4 and FOXO1. The primer sequences used were as follows: KLF4: forward, 3'-TGATGACCTACGTGACCG-5'; reverse, 5'-CCTAACGTAACCTGAATGC-3'; FOXO1: forward, 3'-TGACGAATTCAGACAAGG-5'; reverse, 5'-TCGGAACTACAATTCAAC-3'. β -actin: forward, 3'-GGATCCATGGCATTCCAT-5'; reverse, 5'-TAGCTAGTCGTACATCCGT-3'. Gene expression was normalized to β -actin and calculated using the $2^{-\Delta\Delta CT}$ method.

2.8 Western blotting

Total proteins were extracted from the rats' hippocampal brain tissues, and 20 μg of protein per sample was loaded onto a 10% Sodium Dodecyl Sulfate-Polyacrylamide Gel Electrophoresis (SDS-PAGE) gel for electrophoresis. After separation, the proteins were transferred onto Polyvinylidene Fluoride (PVDF) membranes, blocked with 5% skim milk at room temperature for 2 hours, and the membranes were incubated overnight at 4 $^{\circ}\text{C}$ with primary antibodies against KLF4 (#12173, 1:1000, Cell Signaling Technology (CST), Danvers, MA, USA), FOXO1 (#2880, 1:1000, CST, Danvers, MA, USA), Bax (#5023, 1:1000, CST, Danvers, MA, USA), Bcl-2 (#3498, 1:1000, CST, Danvers, MA, USA) and Cleaved-Caspase-3 (#9664, 1:1000, CST, Danvers, MA, USA). β -actin (#4970, 1:1000, CST, Danvers, MA, USA) was used as the loading control. After three 5-minute washes with Phosphate-Buffered Saline (PBS), membranes were incubated for 1 hour at room temperature with Horseradish Peroxidase (HRP)-conjugated secondary antibody (anti-rabbit IgG, #7074, 1:2000, CST, Danvers, MA, USA). Protein bands were visualized using enhanced chemiluminescence (ECL; Santa Cruz Biotechnology Inc.), followed by autoradiography. The membranes were then scanned, and the band intensities were quantified using the TANON GIS analysis system (GIS 4.0, Tanon Science & Technology, Shanghai, China).

2.9 Terminal deoxynucleotidyl transferase-mediated deoxyuridine triphosphate-biotin nick end labeling (TUNEL) staining

Paraffin-embedded hippocampal brain sections were deparaffinized and rinsed twice with PBS. The sections were then incubated with 3% hydrogen peroxide for 10 minutes to quench endogenous peroxidase activity, followed by treatment with proteinase K working solution for 15–30 minutes. TUNEL staining was performed according to the manufacturer's instructions. After staining, sections were hydrated, permeabilized and sealed with neutral gum. Images were acquired, and the number of apoptotic cells was quantified using ImageJ software. Apoptotic index was calculated as the number of TUNEL-positive cells divided by the total number of cells.

2.10 Morris water maze (MWM) trainings

To acclimate the animals to the test environment, rats in each group underwent 2 hours of free swimming one day before undergoing the MWM training. The Morris Water Maze test was conducted from postnatal days 28 to 35 to assess spatial learning and memory following neonatal SEV exposure and KLF4 knockdown. Their learning ability was evaluated using the navigation test, and memory was assessed using the spatial probe test. In the navigation test, the rats were placed into the water from designated entry points in sequence, and the time taken to locate and climb onto the hidden platform within 2 minutes was recorded as the escape latency. A stable position on the platform for 10 seconds was considered successful platform location; otherwise, the timer continued. For the spatial probe test, the platform was removed, and rats were released into the pool. The time spent in the target quadrant and the number of crossings over the former platform location within 2 minutes were recorded. The search path was also visually analyzed to assess navigation patterns.

2.11 Oxidative stress

The concentration of total protein in brain tissues was determined using the BCA protein assay (A045-4, Jiancheng, Nanjing, Jiangsu, China). Following the manufacturer's instructions, levels of malondialdehyde (MDA; nmol/mg protein), glutathione peroxidase (GSH-Px; U/mg protein), and superoxide dismutase (SOD; U/mg protein) were assessed using corresponding assay kits (A003-1, A005-1 and A001-1, respectively, Jiancheng, Nanjing, Jiangsu, China). For MDA measurement, the protein samples were incubated with the assay reagents at 90 $^{\circ}\text{C}$, followed by centrifugation for 10 minutes. SOD activity was measured by incubating samples with assay reagents at 37 $^{\circ}\text{C}$ for 40 minutes. For GSH-Px measurement, samples were similarly treated at 37 $^{\circ}\text{C}$ and centrifuged for 10 minutes. Absorbance values were measured at the specified wavelengths using a microplate reader (MK3, Thermo Multiskan, Waltham, MA, USA). MDA, a byproduct of lipid peroxidation, serves as a biomarker of oxidative stress resulting from the reaction of reactive oxygen species (ROS) with lipids.

2.12 Dihydroethidium (DHE) staining

ROS generation in brain tissues was assessed using a DHE fluorescence staining kit. DHE is oxidized by intracellular ROS to produce a red fluorescent product that integrates into chromosomal DNA. For this assay, 10 mM DHE was added to unfixed brain sections, followed by incubation for 30 minutes at 37 °C in the dark. The sections were then washed with PBS and mounted using fluorescent mounting medium (S3023, DAKO, Hovedstaden, Denmark). Fluorescence was detected using a fluorescence microscope with excitation/emission filters of 540/25 nm and 605/55 nm, respectively. Fluorescence intensity was quantified using ImageJ software in five randomly selected fields.

2.13 Cell culture and treatment

HT22 cells (American Type Culture Collection, ATCC, Manassas, VA, USA) were cultured in Dulbecco's Modified Eagle Medium (DMEM) supplemented with 10% fetal bovine serum (FBS), 50 µg/mL penicillin and 100 µg/mL streptomycin (pH 7.4) at 37 °C in a humidified incubator containing 5% CO₂. Cells at logarithmic growth phase were seeded in fresh DMEM and cultured for 12 hours prior to treatment. The cells were then exposed to 3% SEV for 2 hours per day for three consecutive days.

2.14 Cell transfection

HT22 cells were divided into five groups: (1) control, (2) control + small interfering RNA (si)-KLF4, (3) SEV + si-NC, (4) SEV + si-KLF4, and (5) SEV + si-KLF4 + si-FOXO1. Small interfering RNAs (siRNAs) targeting KLF4 (si-KLF4) and FOXO1 (si-FOXO1), and a negative control siRNA (si-NC), were purchased from Invitrogen (Carlsbad, CA, USA) and transfected into cells using LipofectamineTM 3000 Transfection Reagent (L3000-008, Invitrogen, Carlsbad, CA, USA) in accordance with the manufacturer's protocol.

2.15 Cell viability measured by CCK-8 assay

HT22 cells were seeded into 96-well plates at a density of 4 × 10⁵ cells/mL, in triplicate wells. After 24 hours of incubation, 10 µL of Cell Counting Kit-8 (CCK-8) solution (C0038, Beyotime, Beijing, China) was added to each well and incubated for an additional 2 hours at 37 °C in the dark. Cell viability was quantified by measuring the absorbance at 490 nm using a microplate reader.

2.16 Flow cytometry analysis

Cells were harvested using 0.25% trypsin (without Ethylenediaminetetraacetic acid), washed twice with PBS at 4 °C, and centrifuged at 1500 rpm for 5 minutes. The cell pellet was resuspended in 100 µL of 1× binding buffer. Subsequently, 5 µL of Fluorescein Isothiocyanate (FITC) and 5 µL of propidium iodide (PI) were added to the suspension, and the cells were incubated for 15 minutes in the dark. After staining, 400 µL of 1× binding buffer was added. The apoptotic rate was measured using flow cytometry.

2.17 DCF testing

Treated HT22 cells were seeded onto laminin-coated glass coverslips. Following adherence, cells were incubated with 1 µmol/L 2',7'-Dichlorodihydrofluorescein diacetate (H₂DCFDA) (D399, Thermo Fisher, Waltham, MA, USA) for 10 minutes. Intracellular ROS levels were visualized by detecting the fluorescence of the oxidized product 2',7'-Dichlorofluorescein (DCF) (S0033, Beyotime, Beijing, China) using a confocal 2D-scanning microscope with a 40× objective lens.

2.18 Statistical analysis

Sample size was determined via power analysis (G*Power 3.1, Düsseldorf, NRW, Germany) based on pilot data, ensuring 80% power ($\alpha = 0.05$) to detect significant effects. Data were assessed for normality (Shapiro-Wilk test) and homogeneity of variance (Levene's test). Normally distributed data were analyzed by one-way Analysis of Variance (ANOVA) with Tukey's *post hoc* test; non-parametric data were analyzed by Kruskal-Wallis test with Dunn's correction. $p < 0.05$ was considered significant. Effect sizes (Cohen's d or η^2) are reported where applicable.

3. Results

3.1 KLF4 expression was elevated and FOXO1 expression was decreased in the hippocampus of neonatal rats treated with 3% SEV

To evaluate SEV-induced nerve injury, modified neurological severity score (mNSS), H&E staining, NISSL staining, and modified Bielschowsky silver staining were performed. As shown in Fig. 1A, rats in the SEV group exhibited significantly higher body righting and negative geotaxis scores compared with those in the Sham group. H&E staining revealed that the hippocampal cells in the Sham group were arranged in an orderly manner, with normal histological features and no apparent damage (Fig. 1B). In contrast, the SEV group showed a marked reduction in the number of hippocampal neurons, along with disorganized cellular arrangement. Some neurons appeared hyperchromatic, with atrophied cytoplasm and enlarged intercellular spaces (Fig. 1C).

Consistently, NISSL staining demonstrated that the hippocampus in the Sham group contained normal, clear, and intact NISSL bodies without evidence of vacuolation. However, in the SEV group, cellular edema was observed, accompanied by diffuse, displaced, and significantly reduced NISSL bodies (Fig. 1D). Moreover, modified Bielschowsky silver staining showed that cortical neurons in the Sham group were large, numerous and regularly arranged (Fig. 1E). The nerve fibers were observed both among cortical neurons and between the cortex and hippocampus. In contrast, the SEV group displayed fewer and smaller cortical neurons, with disorganized arrangement and sparser nerve fibers in both cortical and cortico-hippocampal regions (Fig. 1E). Overall, these findings indicate that 3% SEV exposure induced nerve injury in neonatal rats. Further molecular analyses, including qPCR, immunoblotting,

and immunostaining, revealed elevated mRNA and protein levels of KLF4, along with reduced expression of FOXO1, in the hippocampus of SEV-treated neonatal rats (Fig. 1F–H), suggesting that 3% SEV exposure upregulates KLF4 and downregulates FOXO1 expression in the neonatal rat hippocampus.

3.2 KLF4 knockdown reversed SEV-induced nerve injury in neonatal rats

To further examine the role of KLF4 in 3% SEV-induced nerve injury, KLF4 expression was silenced using shRNA. KLF4 knockdown was initiated 48 hours prior to SEV exposure to ensure effective gene silencing before the primary insult. As shown in Fig. 2A, knockdown of KLF4 significantly reduced its expression in the hippocampus of neonatal rats, while concurrently increasing the expression of FOXO1. H&E staining revealed that KLF4 knockdown had no significant effect on hippocampal structure in the Sham group. In the SEV + AAV-sh-NC group, histopathological features were similar to those observed in the SEV group, indicating that non-targeting control had no protective effect. In contrast, KLF4 knockdown notably alleviated SEV-induced hippocampal injury, as evidenced in the SEV + AAV-sh-KLF4 group (Fig. 2B).

Consistent findings were observed in both NISSL and modified Bielschowsky silver staining. Specifically, knockdown

of KLF4 did not affect neuronal morphology in the Sham group, while it effectively reversed SEV-induced alterations in hippocampal and cortical neurons (Fig. 2C–E). Collectively, these results indicate that KLF4 knockdown mitigates SEV-induced nerve injury in neonatal rats.

3.3 KLF4 knockdown reverses the loss of spatial memory caused by SEV exposure

To evaluate hippocampus-dependent spatial learning and memory, the MWM test was conducted. The swim path patterns are shown in Fig. 3A. Rats in the Sham group exhibited more exploratory and complex swim paths, whereas SEV-treated rats demonstrated simplified navigation patterns, indicating impaired spatial learning. Remarkably, KLF4 knockdown partially restored spatial navigation ability in SEV-exposed rats. Furthermore, SEV exposure led to a significant increase in escape latency, reflecting impaired learning; this effect was reversed by KLF4 knockdown (Fig. 3B). Similarly, SEV exposure decreased the time spent in the target quadrant (Fig. 3C) and the number of platform crossings (Fig. 3D), both of which were restored upon KLF4 silencing. These findings suggest that KLF4 knockdown ameliorates SEV-induced spatial memory deficits in neonatal rats.

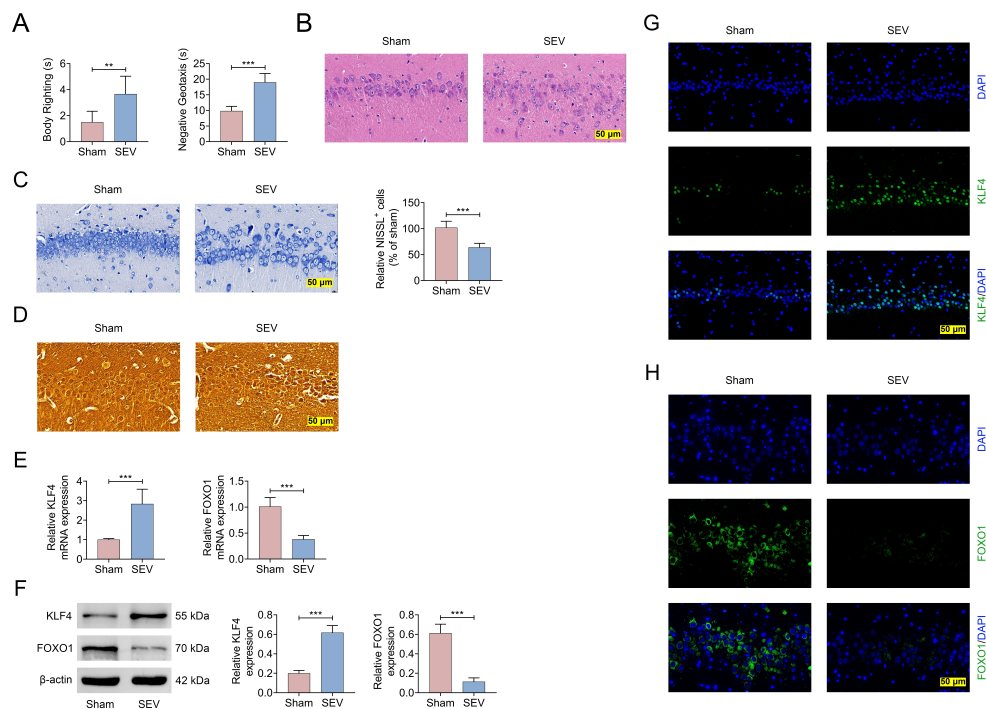


FIGURE 1. KLF4 expression was elevated and FOXO1 expression was decreased in the hippocampus of neonatal rats treated with 3% SEV. Recombinant AAVs were injected intravenously into neonatal rats before SEV exposure with or without 3% SEV treatment. Neonatal rats were divided into two groups: Sham group and SEV group. (A) Body righting and negative geotaxis; (B) Histopathological changes of hippocampus were determined by H&E staining; (C) Nerve injury in hippocampus was measured using NISSL staining; (D) NISSL⁺ cells; (E) Modified Bielschowsky ammonia silver staining was used to evaluate nerve fiber damage in the hippocampus; (F) The mRNA levels of KLF4 and FOXO1 were measured by RT-qPCR; (G,H) The expression of KLF4 and FOXO1 were measured by western blotting and immunohistochemistry. (***p* < 0.01, ****p* < 0.001, Sham group vs. SEV group). SEV: sevoflurane; KLF4: Krüppel-like factor 4; FOXO1: Forkhead box transcription factor O1; NISSL⁺: NISSL-positive; DAPI: 4',6-Diamidino-2-Phenylindole.

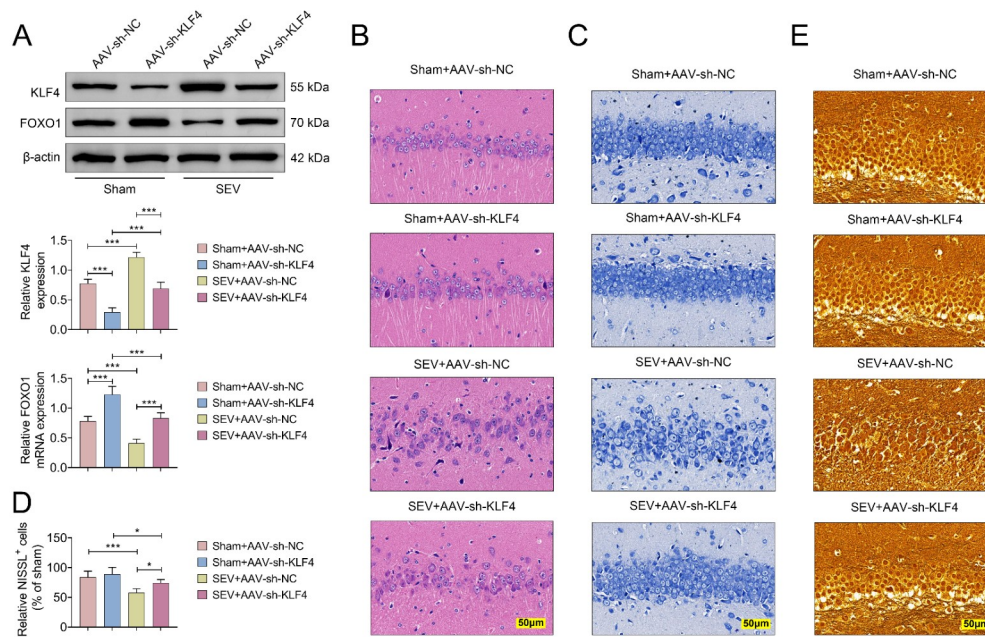


FIGURE 2. KLF4 knockdown reversed SEV-induced nerve injury in neonatal rats. Neonatal rats were divided into four groups: (1) Sham + AAV-sh-NC; (2) Sham + AAV-sh-KLF4; (3) SEV + AAV-sh-NC; (4) SEV + AAV-sh-KLF4. (A) The expression of KLF4 and FOXO1 were measured by western blotting; (B) Histopathological changes of hippocampus were determined by H&E staining; (C) Nerve injury in hippocampus was measured by NISSL staining; (D) NISSL⁺ cells; (E) Modified Bielschowsky ammonia silver staining was used to evaluated nerve fiber damage in the hippocampus. ($*p < 0.05$, $***p < 0.001$, Sham + AAV-sh-NC vs. Sham + AAV-sh-NC or SEV + AAV-sh-NC, or SEV+AAV-sh-KLF4 vs. SEV + AAV-sh-NC or Sham + AAV-sh-KLF4). AAV: adeno-associated virus; KLF4: Krüppel-like factor 4; FOXO1: Forkhead box transcription factor O1; NISSL⁺: NISSL-positive; SEV: sevoflurane; NC: negative control; sh-: Short Hairpin RNA.

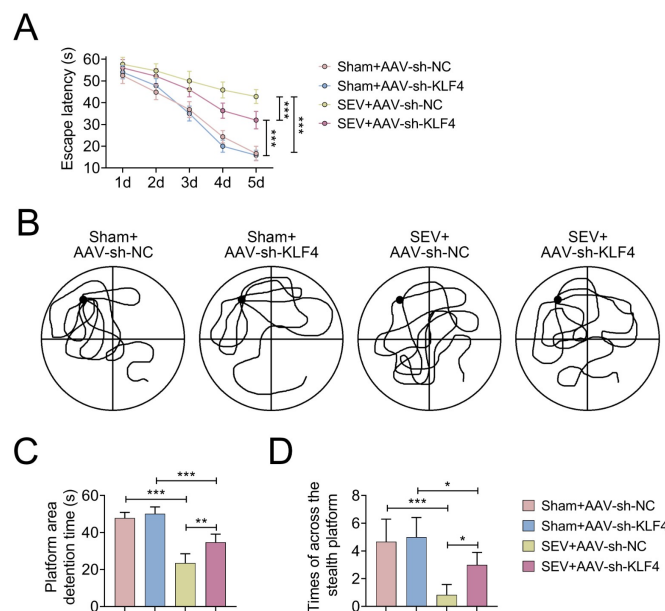


FIGURE 3. knockdown reversed spatial memory loss caused by SEV exposure. Neonatal rats were divided into four groups: (1) Sham + AAV-sh-NC; (2) Sham + AAV-sh-KLF4; (3) SEV + AAV-sh-NC (4) SEV + AAV-sh-KLF4. (A) Representative swimming paths in the MWM test; (B) Escape latency (seconds); (C) Time spent in the target quadrant (seconds); (D) Number of platform crossings ($*p < 0.05$, $**p < 0.01$, $***p < 0.001$, Sham + AAV-sh-NC vs. SEV + AAV-sh-NC, or SEV + AAV-sh-KLF4 vs. SEV + AAV-sh-NC or Sham + AAV-sh-KLF4). AAV: adeno-associated virus; NC: negative control; KLF4: Krüppel-like factor 4; SEV: sevoflurane; sh-: Short Hairpin RNA.

3.4 KLF4 knockdown reversed SEV exposure-induced apoptosis in neuronal cells

To investigate whether KLF4 influences SEV-induced neuronal apoptosis in the hippocampus, TUNEL staining and Western blot analyses of apoptosis-related proteins were performed. As shown in Fig. 4A,B, KLF4 knockdown did not affect neuronal apoptosis in the Sham group. However, SEV exposure significantly increased the number of apoptotic cells, and this effect was reversed by KLF4 knockdown. Western blot results further confirmed these observations. SEV exposure elevated the expression of pro-apoptotic proteins Bax and cleaved caspase-3, while suppressing the anti-apoptotic protein Bcl-2 (Fig. 4C,D). KLF4 knockdown reversed these protein expression changes, suggesting its involvement in apoptosis regulation. Together, these findings demonstrate that

KLF4 knockdown effectively suppresses SEV-induced neuronal apoptosis in the hippocampus.

3.5 KLF4 knockdown reversed oxidative stress induced by SEV exposure

To determine the role of KLF4 in oxidative stress, a series of relevant biochemical assays were performed. SEV exposure significantly elevated MDA levels, while decreasing the activities of SOD and GSH-Px (Fig. 5A). Additionally, ROS levels were markedly increased following SEV treatment, and KLF4 knockdown significantly reversed these effects (Fig. 5B,C), indicating that KLF4 is involved in SEV-induced oxidative stress and that its inhibition exerts a protective effect.

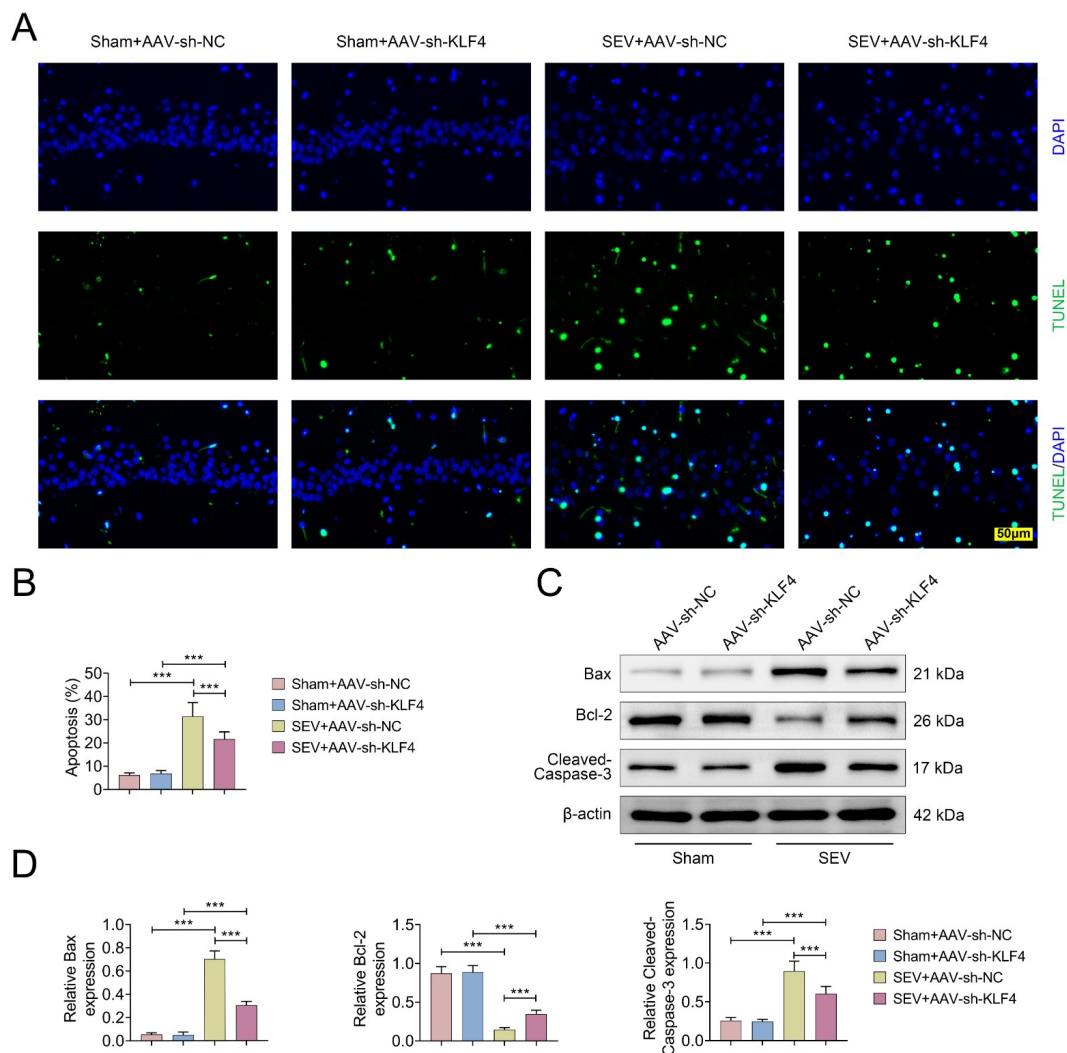


FIGURE 4. KLF4 knockdown reversed SEV exposure-induced apoptosis in neuronal cells. Neonatal rats were divided into four groups: (1) Sham + AAV-sh-NC; (2) Sham + AAV-sh-KLF4; (3) SEV + AAV-sh-NC; (4) SEV + AAV-sh-KLF4. (A) Apoptosis was measured by TUNEL staining; (B) Measurement of apoptosis rate; (C) The expression of Bax, Bcl-2 and Cleaved-caspase 3 measured by western blotting; (D) The expressions of Bax, Bcl-2 and Cleaved-caspase 3 proteins in the four groups analyzed. (***) $p < 0.001$, Sham + AAV-sh-NC vs. SEV + AAV-sh-NC, or SEV + AAV-sh-KLF4 vs. SEV + AAV-sh-NC or Sham + AAV-sh-KLF4). AAV: adeno-associated virus; NC: negative control; KLF4: Krüppel-like factor 4; SEV: sevoflurane; TUNEL: triphosphate-biotin nick end labeling; DAPI: 4',6-Diamidino-2-Phenylindole; sh-: Short Hairpin RNA.

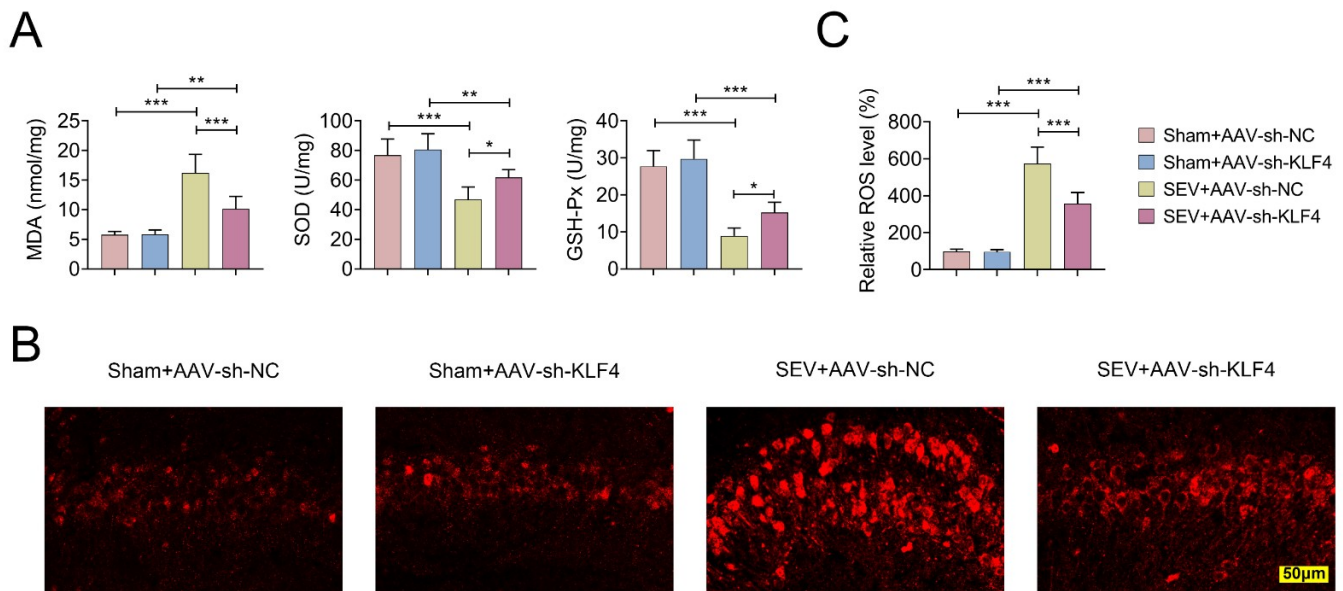


FIGURE 5. KLF4 knockdown reversed oxidative stress induced by SEV exposure. Neonatal rats were divided into four groups: (1) Sham + AAV-sh-NC; (2) Sham + AAV-sh-KLF4; (3) SEV + AAV-sh-NC; (4) SEV + AAV-sh-KLF4. (A) Quantification of oxidative stress markers: MDA, SOD and GSH-Px in hippocampal tissues; (B) ROS levels assessed by DHE fluorescence staining; (C) ROS levels determined using commercial assay kits. (* $p < 0.05$, ** $p < 0.01$, *** $p < 0.001$, Sham + AAV-sh-NC vs. SEV + AAV-sh-NC, or SEV + AAV-sh-KLF4 vs. SEV + AAV-sh-NC or Sham + AAV-sh-KLF4). MDA: malondialdehyde; SOD: superoxide dismutase; GSH-Px: glutathione peroxidase; ROS: reactive oxygen species; AAV: adeno-associated virus; NC: negative control; KLF4: Krüppel-like factor 4; SEV: sevoflurane; sh-: Short Hairpin RNA.

3.6 KLF4 knockdown reversed SEV exposure-induced HT22 cell injury

To further validate the *in vivo* findings, *in vitro* experiments were conducted using HT22 cells. As shown in Fig. 6A, cells in the control and control+si-KLF4 groups maintained normal morphology, characterized by elongated spindle shapes and intact membranes. In contrast, the SEV + si-NC group exhibited pronounced morphological alterations, including cell shrinkage, membrane rupture, and an increased number of floating dead cells. However, KLF4 knockdown (SEV + si-KLF4 group) markedly preserved normal morphology, with fewer damaged or detached cells, suggesting a protective effect against SEV-induced cytotoxicity.

Moreover, *in vitro* analyses confirmed that SEV exposure increased KLF4 expression while suppressing FOXO1 expression in HT22 cells. These effects were reversed by KLF4 knockdown (Fig. 6B). Consistent with this, SEV exposure led to increased apoptosis and elevated oxidative stress in HT22 cells, which were both significantly ameliorated by KLF4 knockdown (Fig. 6C–H). Collectively, these findings demonstrate that KLF4 knockdown mitigates SEV-induced injury in HT22 cells by reducing apoptosis and oxidative stress.

3.7 FOXO1 reversed KLF4-induced apoptosis and increased oxidative stress

To investigate the regulatory relationship between KLF4 and FOXO1, FOXO1 knockdown was performed. Binding site prediction using the JASPAR database identified potential KLF4-binding motifs within the FOXO1 promoter region

(Fig. 7A). As shown in Fig. 7B, FOXO1 expression was significantly elevated following KLF4 knockdown, while subsequent transfection with si-FOXO1 effectively reduced FOXO1 expression levels. Further functional assays revealed that FOXO1 acts downstream of KLF4 and mediates its effects on apoptosis and oxidative stress. Specifically, FOXO1 knockdown abolished the protective effects conferred by KLF4 silencing, resulting in increased neuronal apoptosis and oxidative stress (Fig. 7C–H). These results suggest that FOXO1 plays a key role in counteracting KLF4-induced neuronal injury. In summary, our findings indicate that KLF4 aggravates anesthetic-induced neural damage by negatively regulating FOXO1.

4. Discussion

Anesthesia is widely recognized for its ability to reduce pain, suppress surgical stress, facilitate tolerance to noxious stimuli, and minimize damage to the organism. However, increasing evidence has revealed that anesthetic agents may exert inconsistent biological effects, particularly on neuronal cells. For instance, SEV pretreatment, as well as early post-treatment, reduced cerebral infarction and improved neurological deficit scores in a model of focal cerebral ischemia, potentially through the modulation of mitochondrial Adenosine Triphosphate (ATP)-sensitive potassium channels [20]. In contrast, Lu *et al.* [21] reported SEV-induced neurotoxicity, showing that administration of SEV in 6-day-old neonatal and Alzheimer's disease transgenic mice triggered caspase activation and neuronal apoptosis. Consistent with these findings,

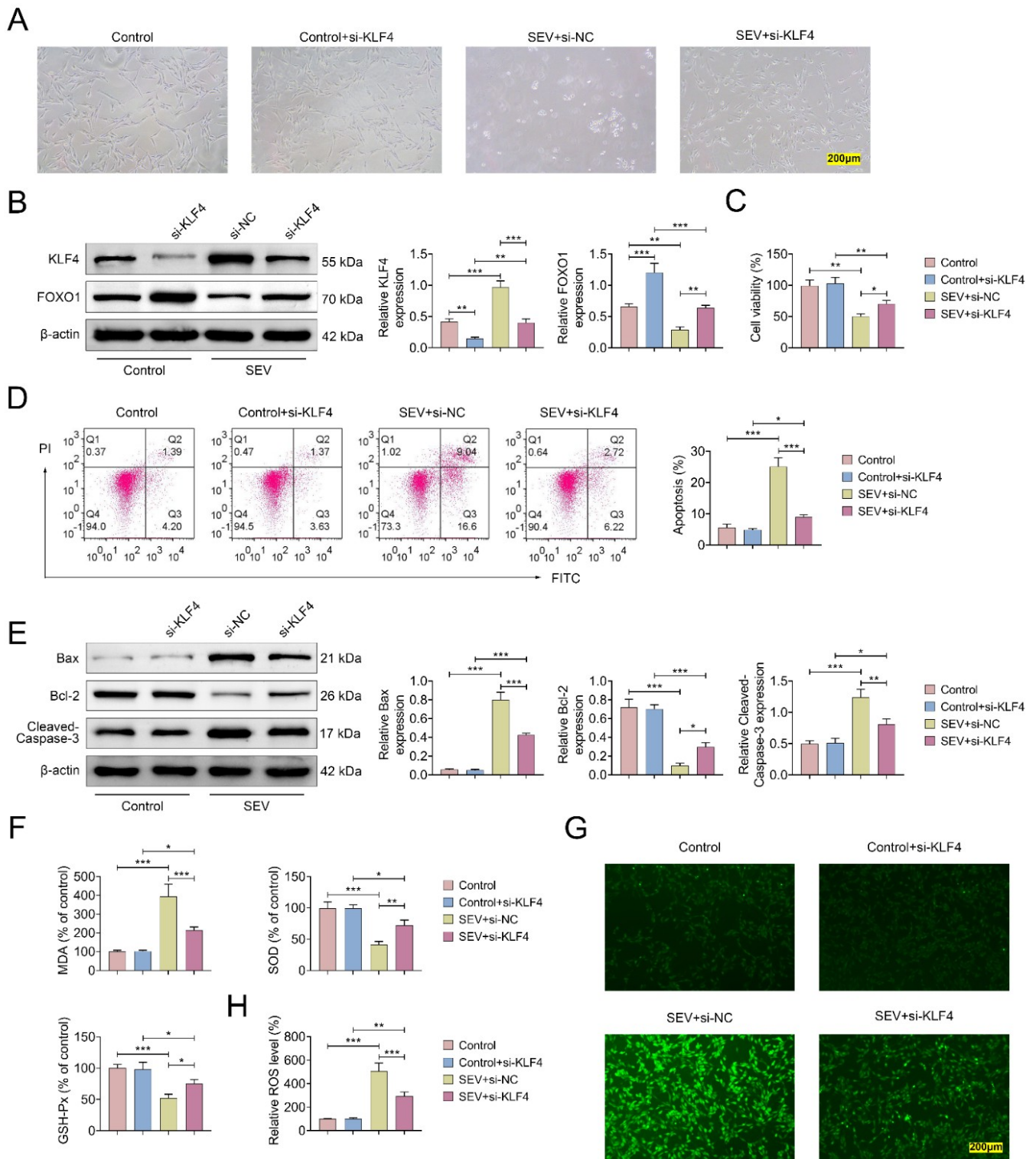


FIGURE 6. KLF4 knockdown reversed SEV exposure-induced HT22 cell injury. HT22 cells were divided into four groups: (1) control; (2) control + si-KLF4; (3) SEV + si-NC; (4) SEV + si-KLF4. (A) Representative cell morphology under light microscopy; (B) Protein expression of KLF4 and FOXO1 analyzed by Western blot; (C) Cell viability assessed using the CCK-8 assay; (D) Apoptosis rate determined by flow cytometry; (E) Expression of apoptosis-related proteins Bax, Bcl-2 and cleaved caspase-3 detected by Western blot; (F) Quantification of MDA, SOD and GSH-Px levels; (G) ROS levels assessed by DCF fluorescence staining; (H) ROS levels measured using commercial assay kits. (* $p < 0.05$, ** $p < 0.01$, *** $p < 0.001$, control vs. control + si-KLF4 or SEV + si-NC, or SEV + si-KLF4 vs. SEV + si-NC or control + si-KLF4). MDA: malondialdehyde; SOD: superoxide dismutase; GSH-Px: glutathione peroxidase; ROS: reactive oxygen species; NC: negative control; KLF4: Krüppel-like factor 4; SEV: sevoflurane; FOXO1: Forkhead box transcription factor O1; PI: propidium iodide; FITC: Fluorescein Isothiocyanate; si-: Small Interfering RNA.

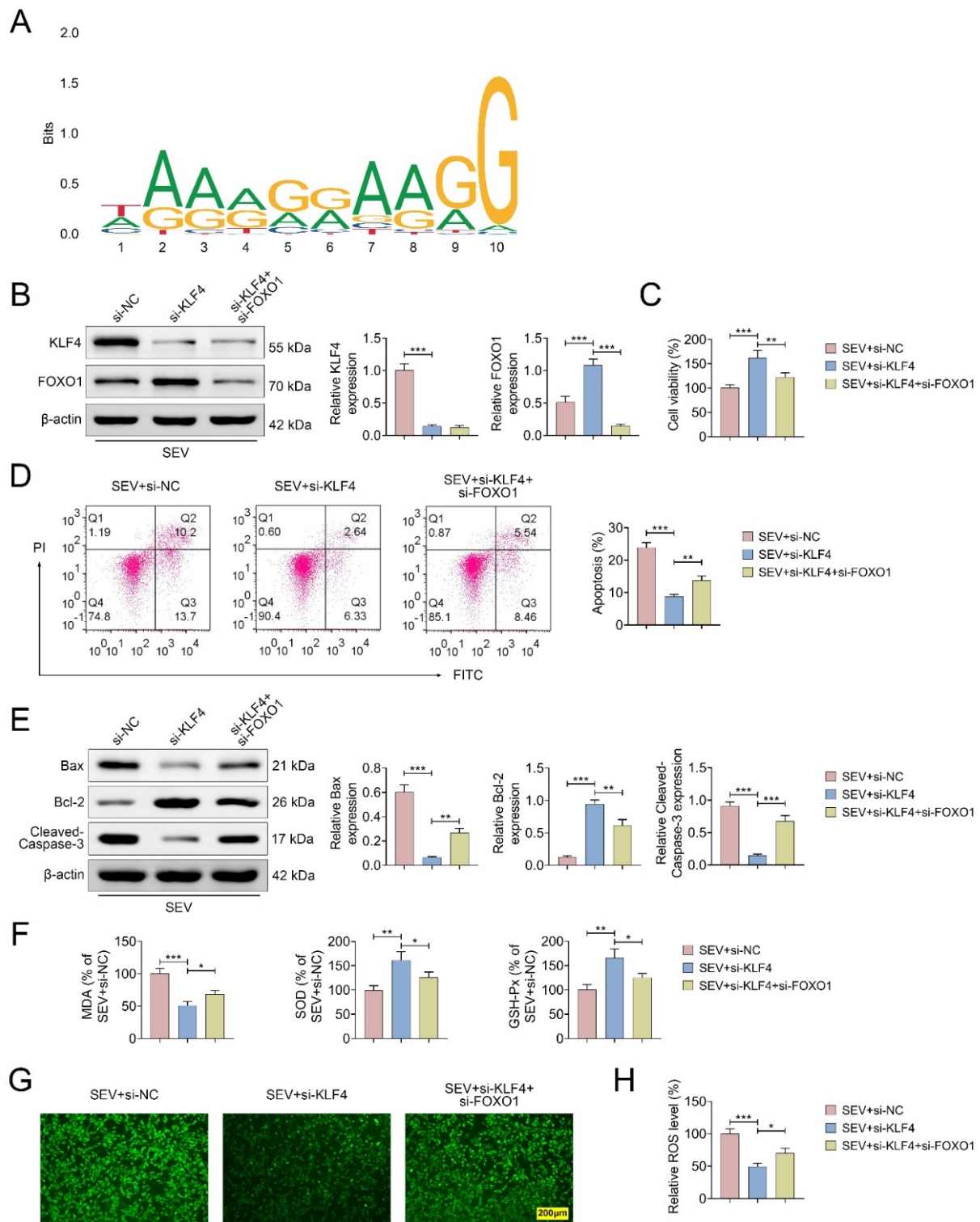


FIGURE 7. FOXO1 reversed KLF4-induced apoptosis and increased oxidative stress. HT22 cells were divided into three groups: (1) SEV + si-NC; (2) SEV + si-KLF4; (3) SEV + si-KLF4 + si-FOXO1. (A) The binding sites of KLF4 binding to FOXO1 were predicted using the JASPAR database; (B) The expression of KLF4 and FOXO1 measured by western blotting; (C) Cell viability was measured by CCK-8; (D) Apoptosis measured by flow cytometry analysis; (E) The expression of Bax, Bcl-2 and Cleaved-caspase 3 measured by western blotting; (F) MDA, SOD, GSH-Px; (G) ROS measured by DCF testing; (H) ROS measured by kits. ($*p < 0.05$, $**p < 0.01$, $***p < 0.001$, SEV + si-KLF4 vs. SEV + si-NC or SEV + si-KLF4 + si-FOXO1). KLF4: Krüppel-like factor 4; FOXO1: Forkhead box transcription factor O1; NC: negative control; SEV: sevoflurane; PI: propidium iodide; MDA: malondialdehyde; SOD: superoxide dismutase; GSH-Px: glutathione peroxidase; ROS: reactive oxygen species; FOXO1: Forkhead box transcription factor O1; FITC-P: Fluorescein Isothiocyanate-Protein; si-: Small Interfering RNA.

our present study revealed that exposure to 3% SEV in neonatal rats resulted in pronounced neurotoxicity, characterized by increased neuronal apoptosis, elevated oxidative stress and impaired learning and memory abilities [22, 23]. These observations support the view that, despite existing inconsistencies in the literature, SEV exposure at this concentration exerts detrimental effects on the developing brain, and the underlying molecular mechanisms warrant further investigation.

Our findings indicated that exposure to 3% SEV exerts a clear neurotoxic effect on neonatal rats. However, the precise molecular mechanisms underlying this toxicity remain incompletely understood. Previous studies have proposed that the developmental neurotoxicity of SEV may involve multiple mechanisms, including nonspecific interactions with N-Methyl-D-Aspartate (NMDA) and Gamma-Aminobutyric Acid (GABA) receptors, as well as disruptions in neuroapoptosis, neurogenesis, and synaptogenesis [24, 25]. Zhang *et al.* [26] reported that SEV impairs cognition in neonatal rats by inducing mitochondrial dysfunction and synaptic loss. Additionally, Dong *et al.* [23] demonstrated that repeated SEV inhalation impairs long-term learning and memory in developing rats by downregulating synapse-associated protein expression, reducing dendritic spine density in the hippocampus, and compromising synaptic plasticity. KLF4, a transcription factor regulated by Enhancer of Zeste Homolog 2 (EZH2), a histone methyltransferase known to exacerbate neurological deficits after ischemic stroke, has emerged as a potential mediator of neuronal injury. EZH2 represses KLF4 expression via direct promoter binding [27]. Previous studies have shown that KLF4 knockdown attenuates nerve injury following Traumatic Brain Injury (TBI) [12]. Nevertheless, the function of KLF4 in SEV-induced neurotoxicity in neonatal rats had not been elucidated. In this study, we established a neonatal rat model of nerve injury induced by 3% SEV to investigate the role of KLF4 in this context. We observed that SEV exposure significantly upregulated KLF4 expression, possibly as a consequence of EZH2 downregulation. Furthermore, our findings revealed that KLF4 upregulation was closely associated with increased neuronal apoptosis, heightened oxidative stress, and impaired learning and memory. These results provide direct evidence for the critical involvement of KLF4 in SEV-induced neural injury and suggest that KLF4 may represent a key molecular target in mitigating anesthesia-associated neurotoxicity during early brain development.

In this study, we focused on investigating the neuroprotective effects of KLF4 knockdown against SEV-induced neural injury and investigated the potential downstream involvement of FOXO1. While we recognize that KLF4 overexpression or FOXO1 knockdown alone under SEV exposure could further strengthen the mechanistic insights, we purposely employed a loss-of-function approach to determine whether suppression of KLF4 alone would be sufficient to alleviate SEV-induced neurotoxicity. Notably, our co-silencing experiments, comparing KLF4 knockdown with or without FOXO1 knockdown, demonstrated that the protective effects of KLF4 silencing were largely dependent on FOXO1, thereby providing compelling functional evidence of a regulatory relationship between KLF4 and FOXO1.

Due to ethical and technical limitations inherent to *in vivo*

studies in neonatal models, KLF4 overexpression was not pursued. Additionally, FOXO1 knockdown alone was not included, as its functional relevance was already evidenced by the attenuation of KLF4 knockdown-mediated protection upon FOXO1 silencing. We believe that the current experimental design offers a focused and adequate demonstration of the role of the KLF4–FOXO1 axis in SEV-induced neurotoxicity.

Our results suggest that KLF4 contributes to SEV-induced neuronal injury, at least in part, by suppressing FOXO1 expression. Nevertheless, considering the broad regulatory functions of KLF4, it is plausible that additional downstream targets and signaling pathways, such as the p53 and JAK/STAT pathways, may also be involved. Further studies are needed to comprehensively elucidate the full spectrum of KLF4-mediated effects in the context of anesthetic-induced neurotoxicity.

Based on these findings, we conclude that KLF4 expression is upregulated in neonatal rats following anesthesia with 3% SEV, and this upregulation is closely associated with SEV-induced neural injury, neuronal apoptosis, oxidative stress, and impaired learning and memory. Previous studies have indicated that KLF4 exerts transcriptional repression on FOXO1 [16], suggesting that elevated KLF4 expression may contribute to the suppression of FOXO1 in neonatal rats after SEV exposure. Supporting this notion, our *in vitro* experiments demonstrated that FOXO1 expression increased following KLF4 knockdown. Notably, FOXO1 overexpression has been shown to reduce oxidative stress and neuroinflammation, thereby attenuating A β production and Tau hyperphosphorylation [28]. As these pathological processes are known to impair synaptic structure and function, they may underlie both early memory loss in Alzheimer's disease and the potential mechanism of SEV-induced developmental neurotoxicity [29]. Consistent with these mechanistic insights, our *in vitro* results revealed that FOXO1 overexpression increased HT22 cell viability and reduced both apoptosis and oxidative stress, suggesting a protective role against SEV-induced neuronal damage.

5. Conclusions

In conclusion, this study used a neonatal rat model of SEV-induced nerve injury to investigate the molecular mechanisms underlying anesthetic neurotoxicity, and the results revealed that SEV exposure could upregulate KLF4 and downregulate FOXO1, leading to neural injury, apoptosis, oxidative stress and cognitive deficits. Furthermore, *in vitro* findings confirmed that KLF4 knockdown increases FOXO1 expression, which in turn enhanced neuronal viability and attenuated apoptosis and oxidative stress. Collectively, this study provides new insights into the molecular basis of SEV-induced neurotoxicity and highlights the regulatory role of the KLF4–FOXO1 axis in this process.

ABBREVIATIONS

SEV, Sevoflurane; KLF4, Kruppel-like Factor 4; FOXO1, Forkhead Box O1; AAV, Adeno-Associated Virus; shRNA, Short Hairpin RNA; NC, Negative Control; MWM, Morris Water Maze; H&E, Hematoxylin and Eosin; RT-

qPCR, Reverse Transcription Quantitative Polymerase Chain Reaction; TUNEL, Terminal Deoxynucleotidyl Transferase dUTP Nick-End Labeling; mNSS, Modified Neurological Severity Score; ROS, Reactive Oxygen Species; DHE, Dihydroethidium; MDA, Malondialdehyde; SOD, Superoxide Dismutase; GSH-Px, Glutathione Peroxidase; CCK-8, Cell Counting Kit-8; DCF, Dichlorofluorescein; PVDF, Polyvinylidene Fluoride; ECL, Enhanced Chemiluminescence; DMEM, Dulbecco's Modified Eagle Medium; FBS, Fetal Bovine Serum; CST, Cell Signaling Technology; KLFs, Krüppel-like factors; SD, Sprague Dawley; NISSL⁺, NISSL-positive; PI, propidium iodide; H₂O₂, hydrogen peroxide; cDNA, complementary DNA; qPCR, Quantitative PCR; SDS-PAGE, Sodium Dodecyl Sulfate-Polyacrylamide Gel Electrophoresis; PBS, Phosphate-Buffered Saline; HRP, Horseradish Peroxidase; EDTA, Ethylenediaminetetraacetic Acid; DAPI, 4',6-Diamidino-2-Phenylindole; C₂H₂, Acetylene; JAK-STAT3, Janus Kinase-Signal Transducer and Activator of Transcription 3; H₂DCFDA, 2',7'-Dichlorodihydrofluorescein Diacetate; DCF, Dichlorofluorescein; ANOVA, Analysis of Variance; si-, Small Interfering RNA; sh-, Short Hairpin RNA; ATCC, American Type Culture Collection.

AVAILABILITY OF DATA AND MATERIALS

All data generated or analyzed during this study are included in this published article.

The datasets used and/or analyzed during the present study are available from the corresponding author on reasonable request.

AUTHOR CONTRIBUTIONS

JJH—designed the study, completed the experiment and supervised the data collection. YFL—analyzed the data, interpreted the data. GQF—prepare the manuscript for publication and reviewed the draft of the manuscript. All authors have read and approved the manuscript.

ETHICS APPROVAL AND CONSENT TO PARTICIPATE

Ethical approval was obtained from the Ethics Committee of Zhongshan Hospital, Fudan University (Approval No. 20221109-002).

ACKNOWLEDGMENT

Not applicable.

FUNDING

This work was supported by the Natural Science Foundation of Xiamen, China (Grant No. 3502Z202374026).

CONFLICT OF INTEREST

The authors declare no conflict of interest.

REFERENCES

- [1] Schifilliti D, Grasso G, Conti A, Fodale V. Anaesthetic-related neuroprotection: intravenous or inhalational agents? *CNS Drugs*. 2010; 24: 893–907.
- [2] Kart PO, Özdemir C, Kayikcioglu T, Cansu A. High-frequency oscillations in self-limited epilepsy with centrotemporal spikes: potential predictors of attention deficit hyperactivity disorder? *International Journal of Developmental Neuroscience*. 2025; 85: e70020.
- [3] Piao M, Wang Y, Liu N, Wang X, Chen R, Qin J, *et al*. Sevoflurane exposure induces neuronal cell parthanatos initiated by DNA damage in the developing brain via an increase of intracellular reactive oxygen species. *Frontiers in Cellular Neuroscience*. 2020; 14: 583782.
- [4] Burnett MG, Zager EL. Pathophysiology of peripheral nerve injury: a brief review. *Neurosurgical Focus*. 2004; 16: E1.
- [5] Jiang J, Tang C, Ren J, Zhang C, Dong L, Zhu Z. Effect of multiple neonatal sevoflurane exposures on hippocampal apolipoprotein E levels and learning and memory abilities. *Pediatrics & Neonatology*. 2018; 59: 154–160.
- [6] Ma R, Wang X, Peng P, Xiong J, Dong H, Wang L, *et al*. α -Lipoic acid inhibits sevoflurane-induced neuronal apoptosis through PI3K/Akt signalling pathway. *Cell Biochemistry & Function*. 2016; 34: 42–47.
- [7] Zhou X, Song FH, He W, Yang XY, Zhou ZB, Feng X, *et al*. Neonatal exposure to sevoflurane causes apoptosis and reduces nNOS protein expression in rat hippocampus. *Molecular Medicine Reports*. 2012; 6: 543–546.
- [8] Wu Z, Xue H, Gao Q, Zhao P. Effects of early postnatal sevoflurane exposure on oligodendrocyte maturation and myelination in cerebral white matter of the rat. *Biomedicine & Pharmacotherapy*. 2020; 131: 110733.
- [9] Shen X, Xiao Y, Li W, Chen K, Yu H. Sevoflurane anesthesia during pregnancy in mice induces hearing impairment in the offspring. *Drug Design, Development and Therapy*. 2018; 12: 1827–1836.
- [10] Qiu J, Zhang Y, Xie M. Chrysotoxine attenuates sevoflurane-induced neurotoxicity *in vitro* via regulating PI3K/AKT/GSK pathway. *Signa Vitae*. 2021; 17: 185–191.
- [11] Pearson R, Fleetwood J, Eaton S, Crossley M, Bao S. Krüppel-like transcription factors: a functional family. *The International Journal of Biochemistry & Cell Biology*. 2008; 40: 1996–2001.
- [12] Cui DM, Zeng T, Ren J, Wang K, Jin Y, Zhou L, *et al*. KLF4 knockdown attenuates TBI-induced neuronal damage through p53 and JAK-STAT3 signaling. *CNS Neuroscience & Therapeutics*. 2017; 23: 106–118.
- [13] Yamamoto H, Uchida Y, Chiba T, Kurimoto R, Matsushima T, Inotsume M, *et al*. Transcriptome analysis of sevoflurane exposure effects at the different brain regions. *PLOS ONE*. 2020; 15: e0236771.
- [14] Zhao Y, Zhang H. Propofol and sevoflurane combined with remifentanyl on the pain index, inflammatory factors and postoperative cognitive function of spine fracture patients. *Experimental and Therapeutic Medicine*. 2018; 15: 3775–3780.
- [15] Fu JB, Wang ZH, Ren YY. Forkhead box O1-p21 mediates macrophage polarization in postoperative cognitive dysfunction induced by sevoflurane. *Current Neurovascular Research*. 2020; 17: 79–85.
- [16] Tang G, Liu D, Xiao G, Liu Q, Yuan J. Transcriptional repression of FOXO1 by KLF4 contributes to glioma progression. *Oncotarget*. 2016; 7: 81757–81767.
- [17] Zhu J, Zhang Z, Jia J, Wang L, Yang Q, Wang Y, *et al*. Sevoflurane induces learning and memory impairment in young mice through a reduction in neuronal glucose transporter 3. *Cellular and Molecular Neurobiology*. 2020; 40: 879–895.
- [18] Ghadge GD, Sonobe Y, Camarena A, Drigotas C, Rigo F, Ling KK, *et al*. Knockdown of GADD34 in neonatal mutant SOD1 mice ameliorates ALS. *Neurobiology of Disease*. 2020; 136: 104702.
- [19] Zhang L, Shen C, Chu J, Zhang R, Li Y, Li L. Icariin decreases the expression of APP and BACE-1 and reduces the β -amyloid burden in an APP transgenic mouse model of Alzheimer's disease. *International Journal of Biological Sciences*. 2014; 10: 181–191.

- [20] Hou Y, Li S, Hou Q, Wang R, Xu X, Li Z, *et al.* Vitamin K2 mitigates cognitive, and motor impairments induced by multiple surgery with anesthesia and analgesia in neonatal stage. *Biochemical and Biophysical Research Communications*. 2025; 765: 151784.
- [21] Lu Y, Wu X, Dong Y, Xu Z, Zhang Y, Xie Z. Anesthetic sevoflurane causes neurotoxicity differently in neonatal naïve and Alzheimer disease transgenic mice. *Anesthesiology*. 2010; 112: 1404–1416.
- [22] Xu Z, Qian B. Sevoflurane anesthesia-mediated oxidative stress and cognitive impairment in hippocampal neurons of old rats can be ameliorated by expression of brain derived neurotrophic factor. *Neuroscience Letters*. 2020; 721: 134785.
- [23] Dong Y, Hong W, Tang Z, Gao Y, Wu X, Liu H. Sevoflurane leads to learning and memory dysfunction via breaking the balance of tPA/PAI-1. *Neurochemistry International*. 2020; 139: 104789.
- [24] Stucke AG, Stuth EA, Tonkovic-Capin V, Tonkovic-Capin M, Hopp FA, Kampine JP, *et al.* Effects of sevoflurane on excitatory neurotransmission to medullary expiratory neurons and on phrenic nerve activity in a decerebrate dog model. *Anesthesiology*. 2001; 95: 485–491.
- [25] Li T, Huang Z, Wang X, Zou J, Tan S. Role of the GABAA receptors in the long-term cognitive impairments caused by neonatal sevoflurane exposure. *Reviews in the Neurosciences*. 2019; 30: 869–879.
- [26] Zhang J, Dong Y, Lining Huang, Xu X, Liang F, Soriano SG, *et al.* Interaction of Tau, IL-6 and mitochondria on synapse and cognition following sevoflurane anesthesia in young mice. *Brain, Behavior, & Immunity-Health*. 2020; 8: 100133.
- [27] Shao H, Dong D, Shao F. Long non-coding RNA TUG1-mediated down-regulation of KLF4 contributes to metastasis and the epithelial-to-mesenchymal transition of colorectal cancer by miR-153-1. *Cancer Management and Research*. 2019; 11: 8699–8710.
- [28] Czapski GA, Cieřlik M, Wencel PL, Wójtowicz S, Strosznajder RP, Strosznajder JB. Inhibition of poly (ADP-ribose) polymerase-1 alters expression of mitochondria-related genes in PC12 cells: relevance to mitochondrial homeostasis in neurodegenerative disorders. *Biochimica et Biophysica Acta. Molecular cell research*. 2018; 1865: 281–288.
- [29] Fan X, Mao X, Yu P, Han D, Chen C, Wang H, *et al.* Sleep disturbance impaired memory consolidation via lateralized disruption of metabolite in the thalamus and hippocampus: a cross-sectional proton magnetic resonance spectroscopy study. *Journal of Alzheimer's Disease*. 2024; 102: 1057–1073.

How to cite this article: Jingjing Hu, Yuanfang Li, Guoqiang Fei. KLF4 promotes sevoflurane-induced neurotoxicity by suppressing FOXO1 expression in neonatal rats. *Signa Vitae*. 2025; 21(6): 111-123. doi: 10.22514/sv.2025.089.